

## **A SIMPLIFIED MODEL FOR PRESSURE DISTRIBUTION IN ELASTIC – PERFECTLY PLASTIC CONTACTS**

**UNGUREANU Ioan, SPINU Sergiu**

University “Stefan cel Mare” of Suceava, ROMANIA

e-mail: ionut@fim.usv.ro, sergiu.spinu @fim.usv.ro

**Keywords:** elasto-plastic contact, problem discretization, conjugate gradient, fast Fourier transform

**Abstract:** A simplified algorithm to predict pressure distribution in elastic – perfectly plastic contacts is advanced in this paper. The model relies on the numerical solution for the elastic contact advanced by Polonsky and Keer, enhanced with Discrete Convolution Fast Fourier Transform (DCFFT) technique to efficiently evaluate convolution products. Contribution of plastic strain region is accounted for indirectly, by imposing a material dependent upper limit for the nodal pressures. The new constriction is imposed during conjugate gradient iterations, thus a new iterative level, present in most elastic – perfectly plastic solvers, is not required. Numerical simulations are performed for several types of contact geometries.

### **1. INTRODUCTION**

The formalism in which analytical solutions of contact mechanics are derived no longer meets the requirements of modern design, in which technological improvements led to more complex surface equations for the contacting bodies. While Hertz model assumes surface around contact region as smooth and quadratic, the surface of any engineering element is inevitably rough. The analysis of roughness-induced stresses was performed mainly using statistical or deterministic models. While statistical theories do not account for the essentially multiscale nature of surface topography, deterministic models require a fine discretization of the contact area, which increases dramatically the computational effort. Consequently, the interest for fast and accurate numerical methods led to important developments in this domain.

Following the works of Mayeur, [8], for the two-dimensional case and of Jacq et al. [5], for the three-dimensional model, elastic-plastic contact problem is solved numerically with algorithms based on multiple levels of iterations. The main idea is to relate elastic and residual part of the solution until convergence is reached. Pressure distribution is related to plastic strain via surface residual displacement. In its turn, plastic strain is related to pressure via contact stresses. This formulation, which determines explicitly the plastic strain region, leads to increased model complexity. One additional drawback is present when modeling contact of elastic - perfectly plastic bodies: the increment of plastic strain cannot be determined from Prandtl-Reuss equations for this type of behavior. Consequently, the residual state cannot be solved using this formulation.

A simplified model, which predicts pressure distribution without computing explicitly the residual state, is presented in this paper. For elastic - perfectly plastic contacts, a limiting value for pressure was observed experimentally or by finite element simulations. Abbott and Firestone, [1], suggested that this value, also referred to as yield pressure, is nearly three times the yield strength of the softer material:  $p_{\max} = 3\sigma_Y$ .

### **2. FORMULATION**

The algorithm newly proposed is centered on the elastic contact solver advanced by Polonsky and Keer, [9], completed with the new constriction which imposes nodal pressures limitation to yield pressure value.

Using Betti's reciprocal theorem, Mayeur, [8], decomposed the elastic-plastic contact problem in an elastic and a residual part, as shown in Fig. 1. The plastic strain is denoted by  $\epsilon^p$  and pressure distribution by  $\mathbf{p}$ . The two problems are not independent, because

solution of the elastic subproblem requires residual deflections, while elastic stresses are needed for the solution of the residual subproblem. The displacements, the strains and the elastic stresses have both elastic and residual components, which are determined in an iterative approach, based on the relation between pressure distribution and plastic strain region.

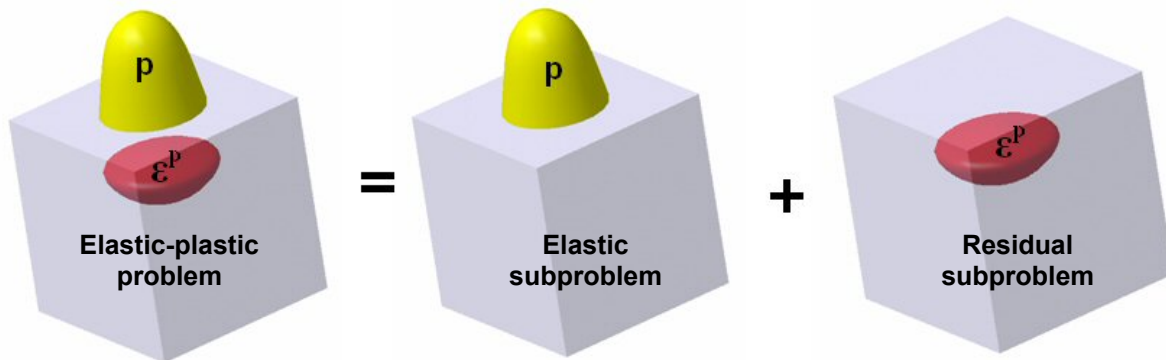


**Figure 1. Decomposition of elastic-plastic contact problem**

According to this formulation and reciprocal theorem, contact interference equation can be written:

$$\mathbf{h} + \omega = \mathbf{u}^{pr} + \mathbf{u}^r + \mathbf{h}i. \quad (1)$$

with  $\mathbf{h}$  the gap between the deformed bodies,  $\mathbf{u}^{pr}$  and  $\mathbf{u}^r$  displacements in the  $z$ -axis direction induced by pressure and by plastic strain respectively,  $\mathbf{h}i$  initial contact geometry and  $\omega$  normal displacement.

Three levels of iterations are employed to solve the resulting model, requiring important computational resources. A simplified approach can be used [10,11], in order to avoid the complexity of the iterative formulation. This is suitable for computing rough contact problems in particular, as pressure spikes induced by surface irregularities are leveled to an imposed limit.

If the load  $W$  transmitted through contact is sampled in small quantities, the loading increments change insignificantly the free surface deflections. Consequently, the term  $\mathbf{u}^r$  in eq. (1), which accounts for the residual subproblem, can be neglected and the problem is reduced to the elastic formulation. However, an upper limit of pressure on the contact area is usually assumed. This limit is related to the elastic – perfectly plastic behavior of the softer material, as a function of the yield strength.

A domain  $D$ , expected to include the contact area  $A$  is chosen. In this domain, contact geometry should be known, or can be extrapolated from existing data. A uniform rectangular grid with non-overlapping interiors is considered in the plane of contact. The elementary cell area is denoted by  $\Delta$ . A Cartesian coordinate system, with  $x$  and  $y$ -axes aligned with the grid directions, having its origin fixed at a grid corner, is attached. Individual nodes are identified by a pair of indices  $(i, j)$ , with  $1 \leq i < N_x$ ,  $1 \leq j < N_y$  and  $N = N_x N_y$ . The nodal value of any continuous distribution  $f(x, y)$  over  $D$  is denoted by  $f_{ij}$ .

The limiting surfaces of the contacting bodies are sampled in two height arrays corresponding to grid control points (usually, elementary cell centroids). Such data can be obtained from an atomic force microscope or an optical profilometer. The sum of the two

heights at node  $(i, j)$  yields the composite surface height  $h_{ij}$ . For the half-space approximation to remain valid, the slope of composite geometry should be small.

The digitized pressure distribution generates deflections in the directions of the inner normals to corresponding surfaces. Normal surface deflections must match in the contact area; in-plane deflections can usually be ignored, according to Johnson, [6]. The bodies in contact being approximated by half-spaces, the deflections are aligned with the  $z$ -axis in all points. The nodal values  $u_{ij}$  can be calculated as a convolution of influence coefficients matrix  $\mathbf{K}$  with pressure  $\mathbf{p}$ . The following conditions must be also verified:

- No interpenetration is allowed:  $h_{ij} \geq 0, (i, j) \in D$ .
- Surface tractions cannot be tensile, only pressures:  $p_{ij} \geq 0, (i, j) \in D$ .
- To account for plastic yielding, an upper limit on the contact pressure is imposed, related to the yield strength of the softer material:  $p_{ij} \leq p_{\max}, (i, j) \in D$ .

This leads to the following discrete formulation of the simplified elastic – perfectly plastic contact problem:

$$h_{ij} = u_{ij} + h_{ij} - \omega, (i, j) \in D; \quad (2)$$

$$W = \Delta \cdot \sum_{i=1}^{N_x} \sum_{j=1}^{N_y} p_{ij}; \quad (3)$$

$$h_{ij} = 0, p_{ij} > 0, (i, j) \in A; \quad (4)$$

$$h_{ij} > 0, p_{ij} = 0, (i, j) \in D \setminus A; \quad (5)$$

$$p_{ij} \leq p_{\max}, (i, j) \in A. \quad (6)$$

The system of equations and inequalities (2)-(6) must be solved in nodal pressures, while the contact area, namely the set of nodes in contact, is also unknown. Both pressure distribution and contact area are determined in course of iteration, by trial-and-error. The adjustment of contact area is performed by exclusion of cells having negative pressures, and by (re)inclusion of overlapping cells (cells with negative gap).

Since the work of Polonsky and Keer, [9], elastic contact problems with arbitrarily contact geometry are solved in a single-loop iterative scheme based on the conjugate gradient method, combined with either MLMS, [2], or DCFIT, [7], for the computation of elastic displacements. In other formulations, [10,11], in order to account for the elastic-plastic behavior, an outer level of iteration, needed to enforce the static force equation (3), is used, resulting in increased computational requirements. The method advanced in this paper does not require an outer level of iteration, the load balance condition being enforced on every iteration by adjustment of nodal pressures.

Before the start of iterations, the following input must be acquired: grid parameters, elastic parameters of involved materials, yield pressure, the accuracy goal for the conjugate gradient iteration.

Initial non-negative values are chosen for  $p_{ij}$ , verifying the force balance condition. The set of nodes for which the pressure is positive form the current contact area  $A$ . The set of nodes with pressures exceeding  $p_{\max}$  is denoted by  $P$ . The following relation holds:

$P \subset A \subset D$ . Auxiliary variables are also initialized:  $\omega = 0$ ,  $R^{old} = 1$ . The influence coefficients matrix  $\mathbf{K}$  is computed from grid parameters and elastic material properties. The following sequences are repeated until the accuracy goal is achieved.

Surface deflections  $u_{ij}, (i, j) \in D$  are computed as a convolution of  $\mathbf{K}$  and  $\mathbf{p}$  over  $D$ . Efficient calculation is available through DCFFT, [7]. The gap distribution is then obtained:

$$h_{ij} = u_{ij} + hi_{ij}, (i, j) \in D. \quad (7)$$

In terms of conjugate gradient formulation,  $\mathbf{h}$  is the residual, namely an indication of how far the current estimation is from the exact solution. At the same time,  $\mathbf{h}$  is the direction of steepest descent and the first descent direction in conjugate gradient iteration. The gap is then normalized by its mean value  $\bar{h}$  over  $A-P$  and the sum  $R$  is computed:

$$h_{ij} \leftarrow h_{ij} - \bar{h}, (i, j) \in D; \quad (8)$$

$$R = \sum_{(i,j) \in A-P} h_{ij}^2. \quad (9)$$

The direction in which the next step will be made is then assessed. In the multidimensional space of pressures  $p_{ij}, (i, j) \in A-P$ , every new descend direction is constructed from the residual, such as it is  $\mathbf{K}$ -orthogonal to all previous residuals and search directions:

$$d_{ij} = \begin{cases} r_{ij} + \varpi \cdot R/R^{old} d_{ij}, (i, j) \in A-P; \\ d_{ij} = 0, (i, j) \in (D-A) \cup P. \end{cases} \quad (10)$$

The value stored in  $R^{old}$  is then updated:

$$R^{old} \leftarrow R. \quad (11)$$

A convolution of  $\mathbf{K}$  with descend direction  $\mathbf{d}$  is computed and normalized by its average value over  $A-P$ . The resulting value  $\mathbf{t}$  is used to derive the length  $\alpha$  of the step to be made in the direction of  $\mathbf{d}$ :

$$\alpha \leftarrow \sum_{(i,j) \in A-P} h_{ij} d_{ij} / \sum_{(i,j) \in A-P} t_{ij} d_{ij}. \quad (12)$$

In the next step, nodal pressures  $\mathbf{p}$  are backed up in  $\mathbf{p}^{old}$  for relative error estimation. The pressures in  $A-P$  are then adjusted:

$$p_{ij} \leftarrow p_{ij} - \alpha \cdot d_{ij}, (i, j) \in A-P. \quad (13)$$

In the next step, all tensile tractions, namely negative pressures, are set to zero. The corresponding nodes are consequently excluded from the current contact area. At the same time, the upper limitation of contact pressure is imposed. The value of contact pressure is limited to that of the yield pressure, which is usually three times the yield strength of the softer material:

$$p_{ij} = p_{max}, (i, j) \in P. \quad (14)$$

The condition of non-overlapping surfaces is used next. Pressures at nodes with vanishing pressure but negative gap are adjusted in the direction of the residual, with a step of size  $\alpha$ , according to (13). With this correction, the corresponding nodes re-enters contact area, as  $-\alpha \cdot d_{ij}$  is always positive. If no nodes satisfying this condition are found, auxiliary variable  $\varpi$  is set to unity, otherwise to zero.

The numerical load is then computed and the pressure distribution is adjusted to satisfy the static force equation.

$$W_n = \Delta \sum_{(i,j) \in D} p_{ij}; \quad (15)$$

$$\mathbf{p} \leftarrow \mathbf{p} \cdot W / W_n. \quad (16)$$

The relative error is then compared with the accuracy goal, deciding if a new iteration must be performed:

$$\varepsilon = \sum_{(i,j) \in A} |p_{ij} - p_{ij}^{old}| / W. \quad (17)$$

### NUMERICAL SIMULATIONS

The newly advanced algorithm was implemented in a C computer code and several pressure distributions were obtained for different contact geometries. Pressure distributions profiles for Hertz contact geometry with elastic and elastic – perfectly plastic behavior were plotted in Fig. 2. In Fig. 3, increasing loads are considered together with the elastic – perfectly plastic model.

The value for the yield pressure was set to 5 GPa. Numerical simulations suggest enlargement of contact area with increasing values of  $W$ .

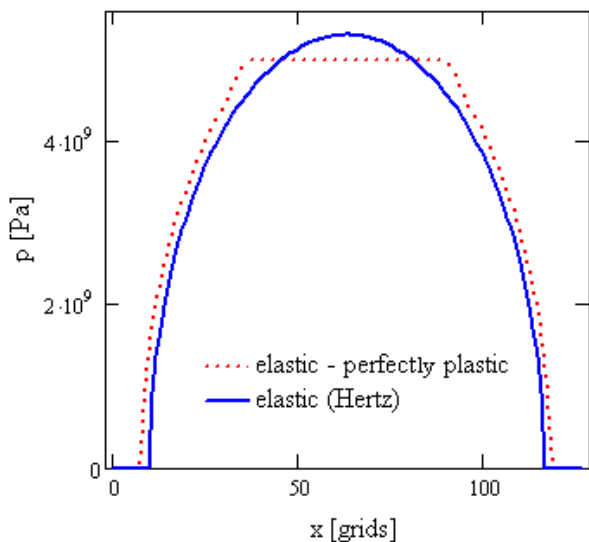


**Figure 2. Elastic and elastic – perfectly plastic behavior for Hertz geometry,  $W = 3600\text{N}$**

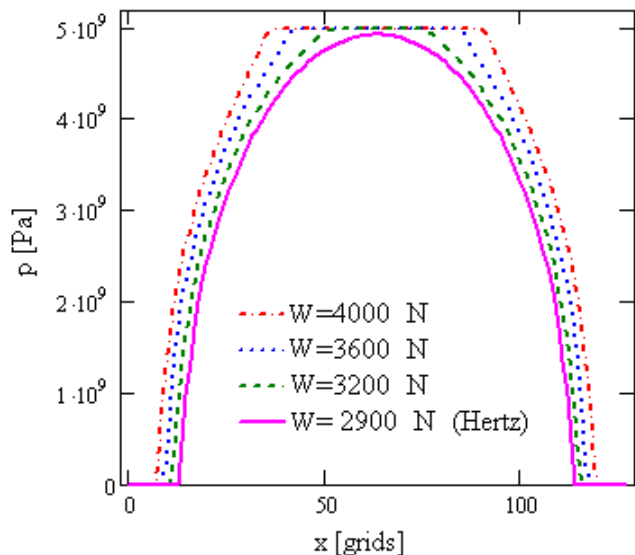


**Figure 3. Elastic – perfectly plastic behavior for Hertz geometry with different loads**

Other types of axisymmetric contacts are considered in the following simulations. A rigid conical indenter with rounded tip is pressed against an elastic - perfectly plastic half-space. The external cone angle is assumed small, so that half-space approximation holds. Closed form expressions for elastic pressure profiles, advanced By Shtaerman, [12], and

by Ciavarella, [3], predict an infinite pressure in the center of the contact when the cone is sharp, and a large, yet finite value, when the cone has a rounded tip. When a limiting value for nodal pressures is imposed, numerical pressure distributions follow the profiles depicted in Fig. 4.

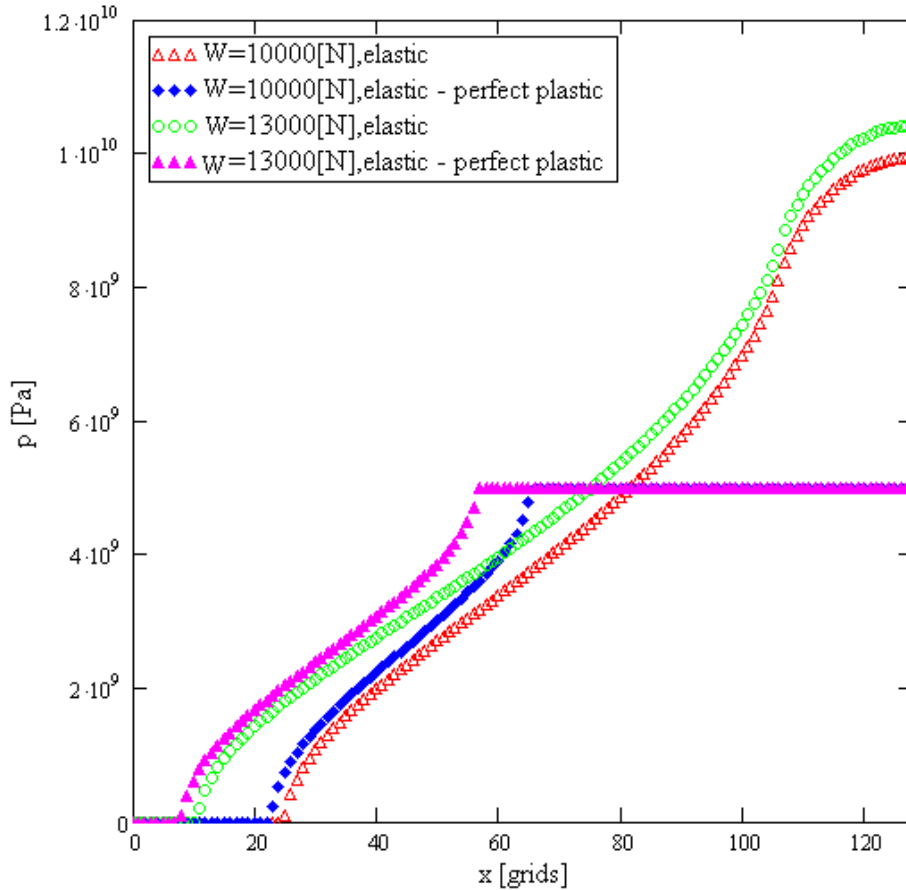


**Figure 4. Elastic and elastic – perfectly plastic contact, conical indenter with rounded tip**

The conforming contact between a circular flat-ended indenter with rounded edge and an elastic – perfectly plastic half-space is simulated in Fig. 5. The pressure risers induced by the edge effect are attenuated by rounding. However, nodal pressures predicted by the purely elastic model exceed the yield strength of the softer material. Elastic - perfectly plastic model is employed to accomplish a more realistic pressure description, as shown in Fig. 5.

All numerical simulations predict that pressure profiles are not smooth at the interface between  $A$  and  $P$ . According to Diaconescu, [4], pressure should be of class  $C^2$  in order to satisfy requirements of the linear theory of elasticity. This condition is not satisfied here, and a smooth pressure profile cannot be obtained using the proposed algorithm.

However, for raw elastic - perfectly plastic models, this formulation may prove to be valuable due to its computational efficiency. Indeed, the speed of convergence of the elastic - perfectly plastic model is of the same order as that of the original purely elastic solver.

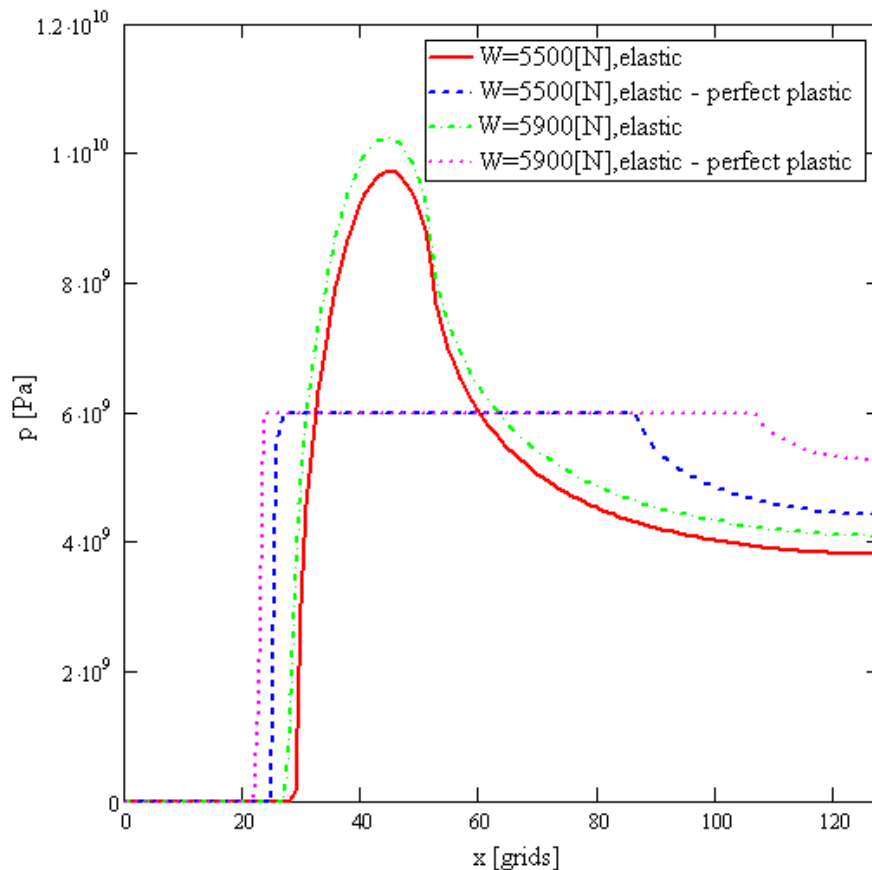


**Figure 5. Elastic and elastic – perfectly plastic contact, flat-ended indenter with rounding radius**

Once pressure distribution computed, the plastic region and the residual stresses can be computed using the compatibility method between elastic and plastic strains, as shown by Popescu, [10], and by Prodan, [11]. Their results suggest that predictions of the simplified formulation for elastic – perfectly plastic contacts match experimental evidences to a high degree of accuracy.

## CONCLUSIONS

A fast numerical method to assess pressure distribution in elastic - perfectly plastic contacts is advanced in this paper. The residual part of displacement, namely contact geometry modification due to plastic flow, is neglected in the interference equation. Consequently, the elastic - perfectly plastic contact problem reduces to the purely elastic case, which can be solved efficiently using an iterative algorithm based on the conjugate gradient method.

Plastic region contribution is accounted for in a simplified manner, by imposing an upper limit for nodal pressures on the contact area, related to the yield strength of the softer material.

The modified conjugate gradient method is almost as fast as the one for the purely elastic case. The greatest decrease in speed of convergence is expected when modeling rough contact.

Three types of axisymmetric contacts are analyzed. A Hertz quadratic indenter, a conical punch with rounded tip and a circular flat-ended indenter with rounding radius are pressed against an elastic-perfectly plastic half-space. In all cases, when assuming elastic - perfectly plastic behavior, an enlargement of contact area is predicted with increased loading.

The obtained pressures distributions can be used to further assess plastic strains and residual stresses in the elastic - perfectly plastic contact, according to compatibility theory between elastic and plastic strains.

## REFERENCES

- [1] Abbott, E. J., and Firestone, F. A., (1933), *Specifying Surface Quality - A Method Based on Accurate Measurement and Comparison*. Mech. Eng. (Am. Soc. Mech. Eng.), 55, pp. 569–572.
- [2] Brandt, A., Lubrecht, A. A., (1990), *Multilevel Matrix Multiplication and Fast Solution of Integral Equations*. J. Comp. Phys 90, pp. 348-370.
- [3] Ciavarella, M., (1999), *Indentation by Nominally Flat or Conical Indenters with Rounded Corners*. Int. J. Solids Struct., 36, pp. 4149-4181.
- [4] Diaconescu, E. N., (1995), *Considerations upon Lundberg Profile*. Acta Tribologica, 3, pp. 7-12.
- [5] Jacq, C., Nelias, D., Lormand, G., and Girodin, D., (2002), *Development of a Three-Dimensional Semi-Analytical Elastic-Plastic Contact Code*. ASME J. Tribol., 124, pp. 653–667.
- [6] Johnson, K.L., (1985), *Contact Mechanics*. Cambridge University Press.
- [7] Liu, S. B., Wang, Q., and Liu, G., (2000), *A Versatile Method of Discrete Convolution and FFT (DC-FFT) for Contact Analyses*. Wear, 243 (1–2), pp. 101–111.
- [8] Mayeur, C., (1995), *Modélisation du contact rugueux élastoplastique*. Ph.D. Thesis, INSA Lyon, France.
- [9] Polonsky, I. A., and Keer, L. M., (1999), *A Numerical Method for Solving Rough Contact Problems Based on the Multi-Level Multi-Summation and Conjugate Gradient Techniques*. Wear, 231(2), pp. 206–219.
- [10] Popescu, G., (1998), *Cercetări teoretice și experimentale privind comportarea în domeniul elasto-plastic a contactelor hertziene fără frecare*, (in Romanian), Ph.D. Thesis, Iași, Romania.
- [11] Prodan, D., (2005), *Cercetări privind contactul circular concentrat al suprafețelor rugoase în domeniul elasto-plastic*, (in Romanian) Ph.D. Thesis, Suceava, Romania.
- [12] Shtaerman, I., (1949), *Contact Problems in the Theory of Elasticity*, (in Russian), Gostehizdat, Moscow.